

**Design and Development of an Experimental Apparatus
to Measure Dynamic Ankle Joint Stiffness of Humans in
Upright Stance**

Honours Undergraduate Thesis

Department of Mechanical Engineering

McGill University Montreal Canada

April 2001

Hank Tun Hon Leung

Table of Contents

TABLE OF CONTENTS	1
TABLE OF FIGURES	4
CHAPTER 1	5
INTRODUCTION AND MOTIVATION	5
1.1 WHY ANKLE?.....	5
1.2 JOINT DYNAMICS.....	7
1.3 APPLICABLE RESEARCH FIELDS.....	7
1.3.1 <i>Control of Upright Stance</i>	7
1.3.2 <i>Orthopaedics</i>	8
1.3.3 <i>Human-Machine Interfaces</i>	9
1.4 MEASURING ANKLE DYNAMIC STIFFNESS	9
1.5 THE NEW EXPERIMENTAL APPARATUS.....	10
1.6 THESIS OUTLINE.....	11
CHAPTER 2	12
ACTUATOR SYSTEM PERFORMANCE REQUIREMENTS	12
2.1 DESIGN REQUIREMENTS OF THE ACTUATING SYSTEM	12
2.2 DYNAMIC ANALYSIS OF ACTIVE TORQUE	13
2.3 DYNAMIC ANALYSIS OF INVOLUNTARY TORQUE.....	13
2.3.1 <i>Inertia Calculations</i>	13
2.3.2 <i>Mathematical Formulation</i>	14
2.3.4 <i>System Model</i>	17
2.3.5 <i>Simulation Results</i>	19
2.3.6 <i>Analysis and Conclusion</i>	25
CHAPTER 3	26
THE DESIGN OF A HYDRAULIC ACTUATING SYSTEM	26
3.1 CHARACTERISTICS OF A HYDRAULIC ACTUATOR.....	26
3.2 HYDRAULIC ACTUATOR SYSTEM.....	26
3.3 CALCULATIONS FOR THE HYDRAULIC ACTUATING SYSTEM	27
3.3.1 <i>Calculations for the Actuator</i>	28
3.3.2 <i>Calculations for the Servovalve</i>	29
CHAPTER 4	34
DETERMINATION OF PUMP SIZE	34
4.1 DISCUSSION OF PUMP SIZE AND ACCUMULATOR	34
4.2 SOLUTION TO THE MINIMIZATION OF PUMP SIZE.....	35
4.3 CALCULATIONS FOR THE SELECTION OF THE HYDRAULIC PUMP	37
4.4 CALCULATIONS FOR THE SELECTION OF THE ELECTRIC MOTOR.....	38
4.5 CONCLUSION	38
CHAPTER 5	40

THE DESIGN OF AUXILIARY COMPONENTS	40
5.1 LIST OF COMPONENTS	40
5.2 TORQUE TRANSDUCERS	40
5.3 POTENTIOMETER	41
5.4 MECHANICAL AND ELECTRICAL STOPS	42
5.5 BEARINGS	44
5.6 FOOT PEDAL AND BRACKET	44
5.7 COUPLINGS	45
CHAPTER 6	48
THE DESIGN OF THE APPARATUS STRUCTURE.....	48
6.1 THE OVERALL DESIGN	48
6.2 SUPPORT FLANGES	49
6.3 BASE	49
6.4 SUBASSEMBLY WITH ACTUATOR, TORQUE SENSOR AND FOOT BRACKET	50
6.5 WHOLE ASSEMBLY WITH FOOT PLATFORM AND HANDRAIL.....	51
REFERENCES	53
APPENDIX	55

Table of Figures

FIGURE 1.0: 3D REPRESENTATION OF ANKLE ROTATION, RANGE OF FREE MOTION (ROM) [2].....	6
FIGURE 1.1: AXIS OF ROTATION OF THE ANKLE, (ROM) [2].	6
FIGURE 2.0: MODEL OF THE BODY.....	14
FIGURE 2.1: BLOCKS REPRESENTING THE BODY-ANKLE MODEL.....	15
FIGURE 2.2: SIMULINK MODEL OF BODY-ANKLE SYSTEM	18
FIGURE 2.3: RESULTS FROM SIMULATION OF HIGH STIFFNESS CASE $K = 1000$ NM/RAD.	20
FIGURE 2.4: RESULTS FROM SIMULATION OF STIFFNESS CASE $K = 1$ NM/RAD.	22
FIGURE 2.5: RESULTS FROM SIMULATION OF LOW STIFFNESS CASE $K = 0.01$ NM/RAD.	23
FIGURE 2.6: ABSOLUTE VELOCITY VS. TORQUE – MAXIMUM CASE AND MINIMUM CASE.....	24
FIGURE 3.0: HYDRAULIC SCHEMATIC OF ACTUATOR AND SERVOVALVE.....	28
FIGURE 3.1: MOOG 72 SERIES SERVOVALVE.....	32
FIGURE 3.2: PERFORMANCE GRAPHS OF MOOG SERIES 72 SERVOVALVE.....	32
FIGURE 4.0: POSITION VS. TIME, VELOCITY VS. TIME – GRAPHS OF THE ACTUATOR.	35
FIGURE 4.1: ABSOLUTE VELOCITY VS. TIME AND ABSOLUTE VELOCITY SUBTRACTED BY AVERAGE VELOCITY VS. TIME.	36
FIGURE 4.2: INTEGRATED VELOCITY (POS) VS. TIME.	37
FIGURE 5.0: LEBOW TORQUE TRANSDUCER 2110-5K.....	41
FIGURE 5.1: MAUREY INSTRUMENTATION MODEL 112-P19 POTENTIOMETER.	42
FIGURE 5.2: ISOMETRIC AND EXPLODED VIEWS OF THE MECHANICAL STOP ASSEMBLY.	43
FIGURE 5.3: PICTURE OF THE LINEAR SENSOR, CAM AND STOP BUTTON.....	44
FIGURE 5.4: ISOMETRIC AND EXPLODED VIEW OF THE FOOT BRACKET AND PEDAL.	45
FIGURE 5.5: TORQUE SENSOR COUPLING.....	46
FIGURE 5.6: ACTUATOR COUPLING.	46
FIGURE 6.0: ISOMETRIC VIEW OF SUPPORT FLANGE.	49
FIGURE 6.1: ISOMETRIC VIEW OF BASE COMPONENT.....	50
FIGURE 6.2: ISOMETRIC VIEW OF SUBASSEMBLY.	51
FIGURE 6.3: ISOMETRIC VIEW OF FINAL ASSEMBLY.	52

Chapter 1

Introduction and Motivation

Standing. A task that is so simple and so natural that it doesn't even require a thought by most people. Yet this seemingly simple task is really a complicated control problem. It requires the coordination of the central and peripheral nervous system to control joint torques to maintain balance and posture. Although we have the basic understanding of the physiology of this task, there are still many unknown details. The goal of this project is to develop an apparatus that will help uncover some of the unknown details of motor control research. One way of accomplishing this is by studying joint dynamics - the dynamic relationship between position of a joint and forces acting about it. This apparatus will be used to measure the ankle joint dynamics of humans in upright stance. And hopefully through the experiments conducted using this machine we can in the future better understand this important task.

In addition to learning how we stand, the knowledge gained from ankle joint dynamics experiments are also very applicable to many other important fields. The following sections will give a brief background to this subject as well as explain the motivation for this project.

1.1 Why Ankle?

First of all, of all the joints in the human body why are we studying the ankle and not any other joints? The reason is because the ankle is an important load-carrying joint in the human body. It is an essential element in maintaining posture and equilibrium of the body. Without ankles we cannot carry out important physical activities such as standing, walking or any type of sports. Thus, it is reasonable to start our investigation of

the joint dynamics at the ankle. And once we have a better understanding of the workings of the ankle, we can then extrapolate those results for the rest of the joints in the human body.

Another reason studying joint dynamics of the ankle is the feasibility of approximating the movement of the ankle as a pure rotation. The ankle rotates about an oblique transverse axis which can be approximated by a line joining a point five cm distal to the medial malleolus to a point three cm distal and eight cm anterior to the lateral malleolus [1]. The figure below gives a 3-D picture of the rotation of the ankle.

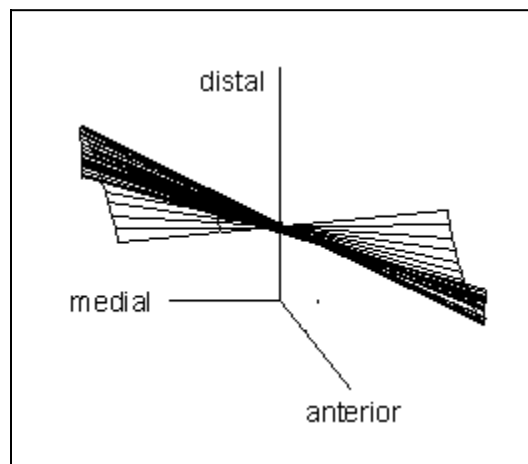


Figure 1.0: 3D Representation of ankle rotation, range of free motion (ROM) [2].

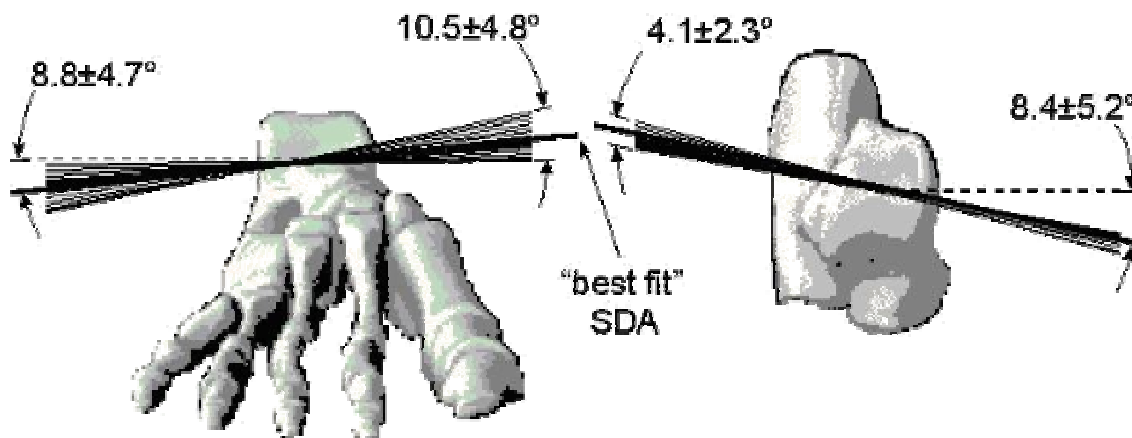


Figure 1.1: Axis of rotation of the ankle, (ROM) [2].

Figure 1.0 and 1.1 shows that although the ankle rotates about an oblique transverse axis, the range of motion away from a pure rotation is small. The proper foot mounting and correct alignment of the axis of rotation of the apparatus with the axis of rotation of the ankle will allow for good experimental results.

1.2 Joint Dynamics

The correct setup of an ankle on its axis of rotation allows for accurate measurement of the position change. This is an important part of the measurement of joint dynamics. The mechanical behaviour of a joint may be defined by its dynamic stiffness – the dynamic relation between its position and the torque acting about it. Dynamic stiffness characterizes the interactions of a joint with the associated limbs and the environment. It is important in the control of posture because stiffness determines the resistance to an external perturbation before voluntary intervention. Stiffness is also important during the execution of movements as it defines the properties of the load that the central nervous system must control. The objective of this project is therefore to construct an apparatus capable of measuring the torque and position of the ankle joint and thus allow for a description of the dynamic stiffness of the ankle.

1.3 Applicable Research Fields

1.3.1 Control of Upright Stance

The study of joint dynamics has many applications. One of the aims of this project is to develop an apparatus that will allow experimentation to further study the role of ankle stretch reflexes in the control of upright stance. Previous studies have examined how proprioceptive, vestibular and visual information are integrated to generate a coordinated response to postural perturbations. In the anterior posterior direction, responses depend on the magnitude of the perturbation. Large inputs evoke responses primarily of the hip rotation –“hip strategy”[3,4,5]. Smaller inputs cause response

primarily in the ankle muscles, which as a result, causes the body to move as an inverted pendulum.

Fitzpatrick et al [5,6,7] studied this ankle strategy in their postural control dynamics experiments by directly applying random forces to the hip and applying linear system identification methods. They concluded that ankle mechanisms were important to the control of stance and could stabilize the body entirely [5,8]. This ankle strategy case will be explored in more detail using this experimental apparatus.

In addition to the basic study of ankle intrinsic and reflex mechanisms in relation to maintaining balance and posture of standing subjects, the adaptation of intrinsic and reflex contributions towards different functional requirements will be examined. Examples types of experiments that explore different functional requirements are tests with/without vision, with/without external support, on different support surfaces and with added loads. These experiments may help with the understanding of the neuromuscular control for balance and posture by isolating the different neuromuscular mechanisms responsible for balance and posture.

1.3.2 Orthopaedics

Another relevant research field is the subject of orthopaedics, in particular, ankle dysfunction. Several diseases and injuries are known to impair the normal function of the ankle joint. These ankle dysfunctions are characterized by symptoms such as spasticity, rigidity, hypertonia, and “stiffness” [9]. The dysfunctionality is manifested in an increased resistance to passive movement, a decrease in the strength of the associated muscles and ligaments, and a declination in the range of free motion.

The quantitative measurement of the joint function will allow for better perception of the progress or recession of a disease or injury. Current clinical qualitative measurements are subjective and inconsistent. As an example, the manual test which is widely employed to evaluate muscle strength, judges the strength of the muscle by its ability to overcome gravity load throughout its range of motion. It is known, however, that nearly half of the extremities muscles show an insignificant change in performance in response to a gravity load; hence such a method lacks consistency [10]. Another

example is Goniometry, which is the measurement of the range of motion of the ankle with a protractor-like instrument. This method is subject to measurement error in reading the scale and in positioning of the instrument. Moreover, it neglects the dynamic effects on the free range of motion [10].

The experimental apparatus developed in this project can be used to provide a quantitative and repeatable measure of ankle joint function. The ability of this apparatus to take measurements from both ankles can lead to comparison of joint functionality between functional and dysfunctional ankles of the same person.

1.3.3 Human-Machine Interfaces

A better understanding of ankle joint dynamics can also aid in the improvement of control systems for robotics and tele-operations. Joint stiffness can be modulated over a wide range by changes in neural activation and consequently it has been proposed that the nervous system modulates muscle [5,11,12], joint [5,13,14,15,16] or endpoint [5,17] stiffness to compensate for external perturbations and/or to initiate voluntary movements. The research in stiffness control has already been implemented for robotic manipulators, thus further knowledge of dynamic joint stiffness continue to improve the control in the area of robotics.

The dynamic joint stiffness experiments conducted by this apparatus will be related to the pedal control aspect of human-machine interfaces; helping develop better and more accurate foot pedal controls of the future.

1.4 Measuring Ankle Dynamic Stiffness

In order to utilize the dynamic joint stiffness knowledge for the potential applications of dynamic joint stiffness discussed in the sections above, it is necessary to first measure and quantify the dynamic joint stiffness. This next section will cover how dynamic joint stiffness is measured. The dynamic joint stiffness was defined above as the dynamic relation between the position and the torque acting about the joint.

Therefore, the device must be able to measure those two mechanical parameters of the ankle: the position of the ankle joint rotation and the torque acting about the ankle joint.

Researchers at the Biomedical Engineering Department at McGill University have already had much experience measuring these two mechanical parameters of the human ankle using their current experimental apparatus. The apparatus that comprises of an electro-hydraulic actuator that induces stochastic perturbations in the ankle joint about a sequence of joint angles spread over the range of motion. A servo-valve, interfaced to a computer controls the position of the actuator. A band limited white noise signal generated by the Matlab software serves as an input displacement signal to the actuator. A high-resolution potentiometer monitors angular position, and a sensitive reaction torque transducer measures the resulting system torque. The output signals of position and torque are then correlated and analyzed using system identification techniques to give a model of ankle dynamic joint stiffness.

The subject's foot is encased in a rigid, individually constructed fibreglass cast that is bolted to a foot bracket attached to the actuator shaft.

The use of a stochastic signal as opposed to a sinusoidal one lies in the fact that the predictability of the input could result in voluntary inflection of muscular activity [18]. Moreover, the periodicity of the input might induce nonlinearities in the response [19]. The presence of nonlinearities in the mechanical properties of the ankle joint necessitated the use of position, rather than torque, as the input and control signal in the system.

1.5 The New Experimental Apparatus

The objective of this project is to design a new experimental apparatus that will allow the measurement of the dynamic ankle stiffness of both ankles of humans in upright stance. The new apparatus will be developed using methods similar to the current experimental apparatus in REK lab. Subjects will stand with each foot on a separate, rotating platform whose axis of rotation is aligned with that of the subject's ankle. Each platform will be under a separate servo control and instrumented to measure the angular position and torque.

1.6 Thesis Outline

This thesis describes the design of the new apparatus. The chapters will follow the development process, from determination of system parameters to the selection of parts to the CAD design.

Chapter 2 will cover the determination of the actuator system performance requirements.

Chapter 3 will cover the calculations that led to the particular selections of the hydraulic rotary actuator and the servovalve.

Chapter 4 will discuss the process of determining the appropriate pump and motor size for the hydraulic power supply of the apparatus.

Chapter 5 will discuss the selection and design of the various auxiliary components of the apparatus.

Finally, in Chapter 6 the overall design of the apparatus, including the different elements of the apparatus, the support frames, the subassemblies and the final assembly will be dealt with.

Chapter 2

Actuator System Performance Requirements

The first part to the design of this experimental apparatus is to determine the operational parameters of the actuating system. This involves the determination of important design parameters such as system bandwidth, torque, angular velocity, angular acceleration, and the variation of these parameters under varying experimental conditions.

2.1 Design Requirements of the Actuating System

The design requirements are based on the operational requirements needed to conduct experiments on the ankles of standing humans. The actuating system must possess the following characteristics:

- 1) The system is capable of imposing random perturbations of ankle position about a series of mean ankle positions spread over the range of motion.
- 2) The system should have a frequency response such that it is adequate for system identification purposes at frequencies higher than the ankle natural frequency. The natural frequency of the ankle can reach 40Hz at high levels of muscle contraction.
- 3) The system can generate adequate torque to perturb the system. The total torque consists of two components. The first component is an involuntary torque due to the passive mechanics encountered during angular perturbations of the ankle joint

including the effects of the inertia of the body. The second component is the active torque generated by voluntary contractions of the associated ankle muscles.

Based on apparatus developed previously in the lab, the components that are required for the actuating system consist of:

- 1) Hydraulic actuators (2): used to deliver position perturbations to ankle joint.
- 2) Servovalve (2): controls the flow and movement of the hydraulic actuator.
- 3) Connector: connects the hydraulic actuator to the servovalves.

The rest of the chapter will set the performance requirements and will be used to select the appropriate hydraulic actuator and servovalve.

2.2 Dynamic Analysis of Active Torque

Active torque is the torque generated by contraction of associated ankle muscles. The maximum voluntary contractions (MVC) of the associated muscles can reach a torque of 150 Nm lasting for 5 seconds and dropping steadily thereafter to reach 25% of the MVC. This value can be maintained throughout the experiment. The steady torque will be taken to be approximately 40 Nm.

2.3 Dynamic Analysis of Involuntary Torque

2.3.1 Inertia Calculations

This apparatus involves perturbation of the ankles of a standing subject. This perturbation during the operation of the apparatus will result in slight displacements of the body with respect to the vertical. This movement can induce added torque on the actuating system. In order to model the mechanics of the body, the inertia of the body must be determined.

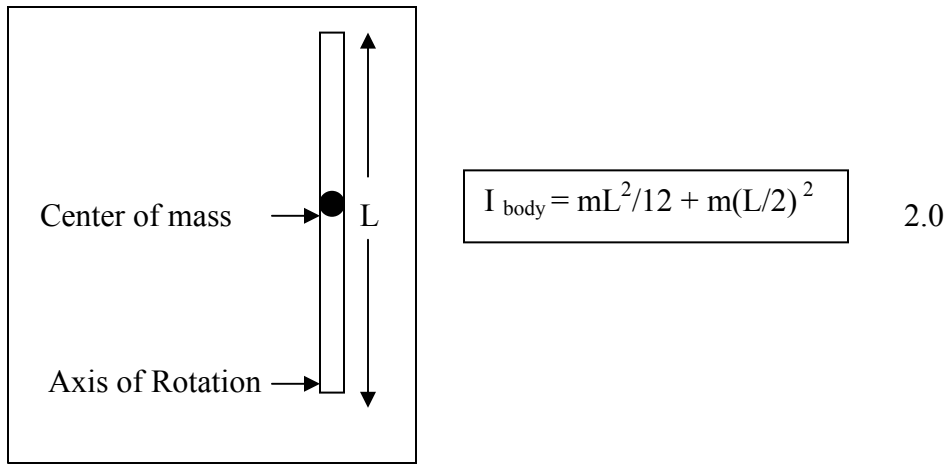


Figure 2.0: Model of the body.

The inertia of the body is modeled using a long rod, assuming that the center of mass of the body is in the middle of the rod. Using Equation 2.0 and taking the characteristics of a typical subject to have a mass $m = 77$ kg and height of $L = 1.8$ m, the inertia of the body is calculated to be $I_b = 83.16 \text{ Kg}\cdot\text{m}^2$.

The inertia of the ankle is also required and from previous researcher's calculation using similar a method was determine to have a value of $I_a = 0.015\text{Kg}\cdot\text{m}^2$.

2.3.2 Mathematical Formulation

Previous researchers have discovered that when operating conditions remain almost constant, the dynamic stiffness of many joints including the wrist, knee, and ankle are described well by linear dynamic models whose parameters vary with the operating point. They modeled the ankle joint as an under damped second-order system where the joint torque is related to inertial, viscous, and elastic components [18,20]. In this model, the involuntary torque generated by angular perturbation of the ankle is represented by:

$$I\ddot{\theta} + B\dot{\theta} + k\theta = T \quad 2.1$$

$T =$ ankle torque (Nm)

B = viscous parameter (Nms/rad)

k = elastic parameter (Nm/rad)

$\ddot{\theta}$ = angular acceleration (rad/s²)

$\dot{\theta}$ = angular velocity (rad/s)

θ = angular position (rad)

The torque given by Equation 2.1 is the result of the passive mechanics of the ankle. This model is unsuitable for the apparatus of standing subjects because it does not consider relationship between the body and the ankle.

A new mechanics model is needed to model the passive mechanics of the ankle as well as the body. The reason for this is because as the body is perturbed and moves in relation with the ankle with respect with the vertical, the effect is a change in the position of the muscles. This movement will generate a passive torque. This effect can be more clearly demonstrated when the ankle body system is translated into the Cartesian coordinate system. The relative position difference between the body and ankle is represented by the difference between position x_1 and x_2 . The ankle and body system is modeled using an equivalent block system: two blocks representing the inertia of the ankle and body respectively and a spring and a damper component to represent the associated muscles. The equations are given below:

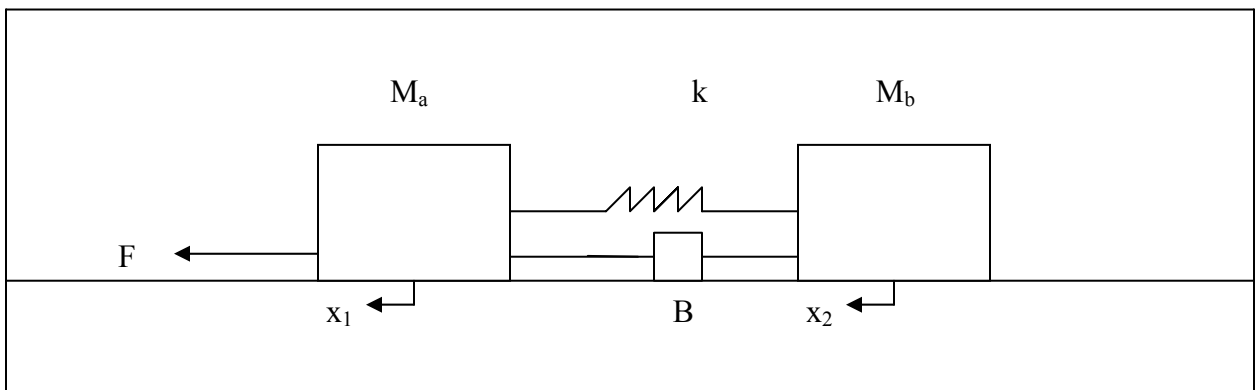


Figure 2.1: Blocks representing the Body-Ankle model.

$$\begin{aligned}
M_a \ddot{x}_1 + B(\dot{x}_1 - \dot{x}_2) + k(x_1 - x_2) &= F \\
M_b \ddot{x}_2 + B(\dot{x}_2 - \dot{x}_1) + k(x_2 - x_1) &= 0
\end{aligned}
\tag{2.2}$$

The above equations can be converted to rotational system:

$$\begin{aligned}
I_a \ddot{\theta}_1 + B(\dot{\theta}_1 - \dot{\theta}_2) + k(\theta_1 - \theta_2) &= T \\
I_b \ddot{\theta}_2 + B(\dot{\theta}_2 - \dot{\theta}_1) + k(\theta_2 - \theta_1) &= 0
\end{aligned}
\tag{2.3}$$

I_a = inertia of the ankle = 0.015 (Kg-m²)

I_b = inertia of the body = 83 (Kg-m²)

B = viscous parameter (Nms/rad)

k = elastic parameter (Nm/rad)

$\ddot{\theta}_1$ = angular acceleration of ankle with respect to the vertical (rad/s²)

$\dot{\theta}_1$ = angular velocity ankle with respect to the vertical (rad/s)

θ_1 = angular position ankle with respect to the vertical (rad)

$\ddot{\theta}_2$ = angular acceleration of body with respect to the vertical (rad/s²)

$\dot{\theta}_2$ = angular velocity body with respect to the vertical (rad/s)

θ_2 = angular position body with respect to the vertical (rad)

Equations 2.3 allows for the modeling of both the ankle and the body. The displacement of the ankle θ_1 is a known value of random position between ± 0.1 radian. The displacement of the body θ_2 is the movement of the body as the ankle is perturbed by θ_1 . A relationship between θ_2 and θ_1 is needed to determine the effects of the displacement of the body on torque. Taking the Laplace of the second equation the relationship between θ_2 and θ_1 is evaluated to be:

$$\theta_2 = \theta_1 \frac{[Bs + k]}{[I_b s^2 + Bs + k]} \quad 2.4$$

Equation 2.4 demonstrates the effect of the elastic component k on the displacement of the ankle and body and consequently on the torque generated. In the case when the ankle becomes infinitely stiff, the elastic component k becomes very large and from the above equation $\theta_2 = \theta_1$. As a result, both the bodies will be moving together with respect to the vertical and the inertia of the body would be in effect. On the contrary if the elastic component k becomes very small, the ankle would be moving free of the body thus the effects of the inertia of the body I_b becomes negligent.

Due to the fact that the stiffness k of the ankle is indeterminate, this dynamic analysis is based the three cases. First case assuming stiffness k is very large, second case assuming stiffness $k \approx 1$, and third case assuming stiffness k is small.

2.3.4 System Model

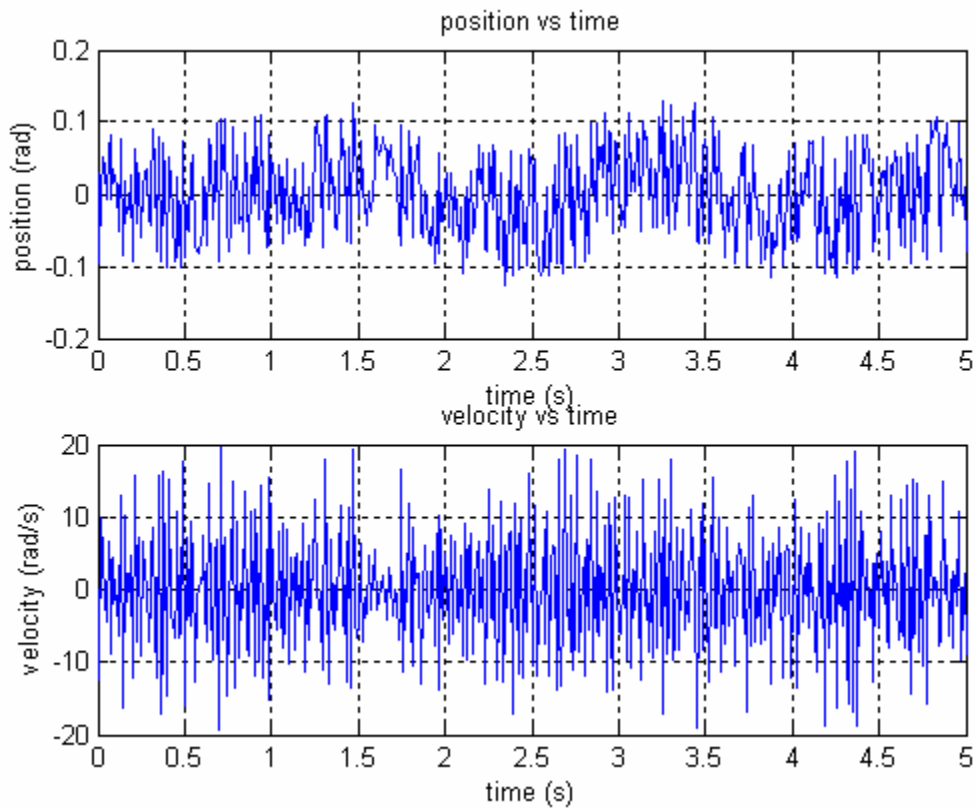
The body and ankle represented by Equations 2.3 and 2.4 were modeled using Matlab Simulink to determine the system characteristics. The position signal is generated using the Signal Generator in Simulink. The signal is a stochastic signal limited at ± 0.1 radians at a frequency of 50 Hertz. This is the same type of input that is to be used in actual experiments. In fact, with Matlab 6.0 and new control software, the Simulink model can be used to directly control the actuator and servovalve. Consequently, the inputs used in this model will be the exact same input used to control the apparatus in future experiments.

The inertial component of Equation 2.3 was determined in Section 2.3.1. The viscous parameter B of Equation 2.3 was determine by earlier experimenters and set at B

2.3.5 Simulation Results

The results below are from the Simulink model above. The displacement of the ankle θ_1 is a known value of random position between ± 0.1 radian that is generated with the random signal generator in Simulink. The position of θ_2 is determined using the Laplace transfer relationship between θ_1 and θ_2 . The position-time, velocity-time, acceleration-time, torque-velocity relationships of the passive mechanics of the ankle and body are shown below for different cases of stiffness:

Case 1: Ankle with high stiffness ($k=1000$)



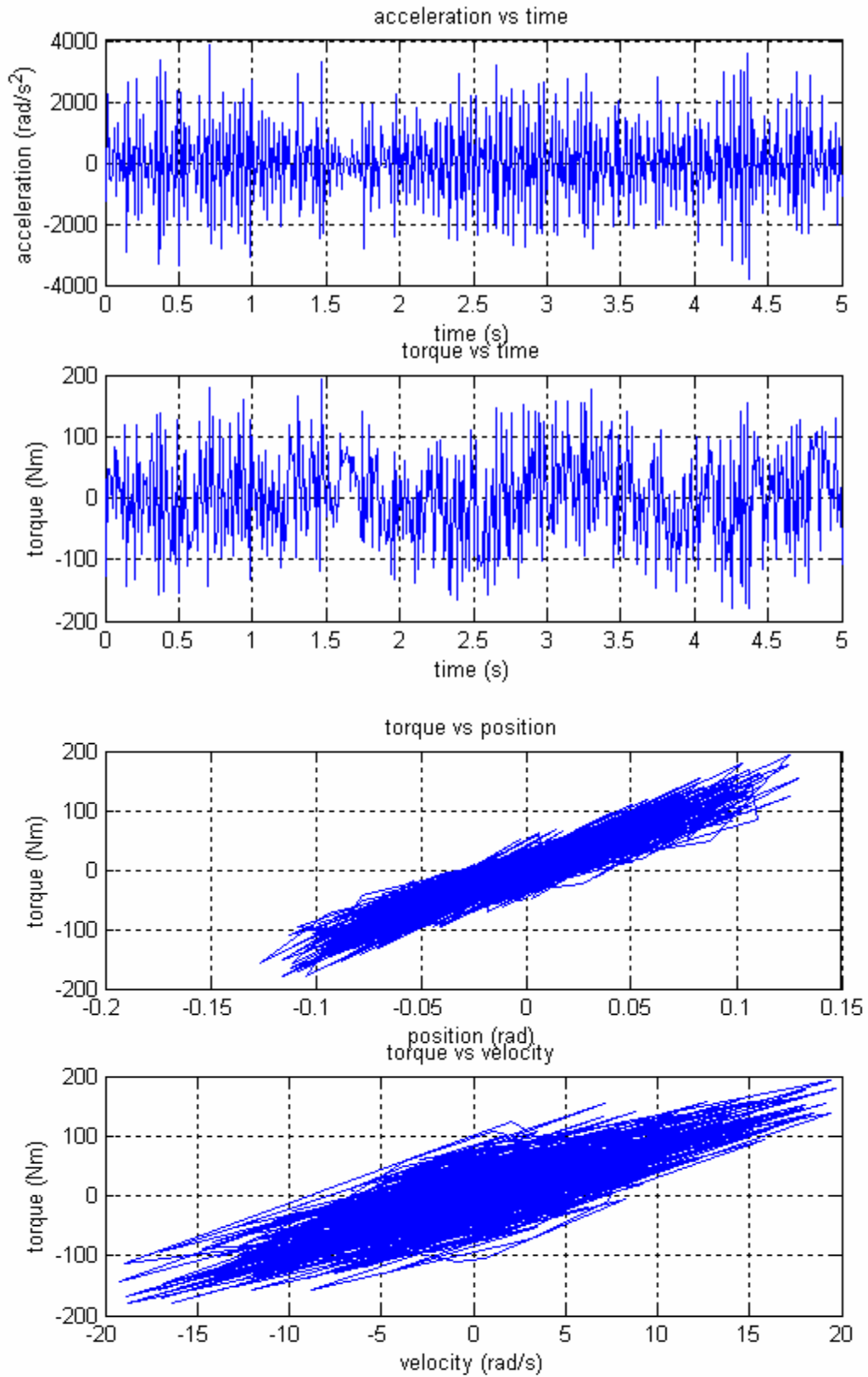
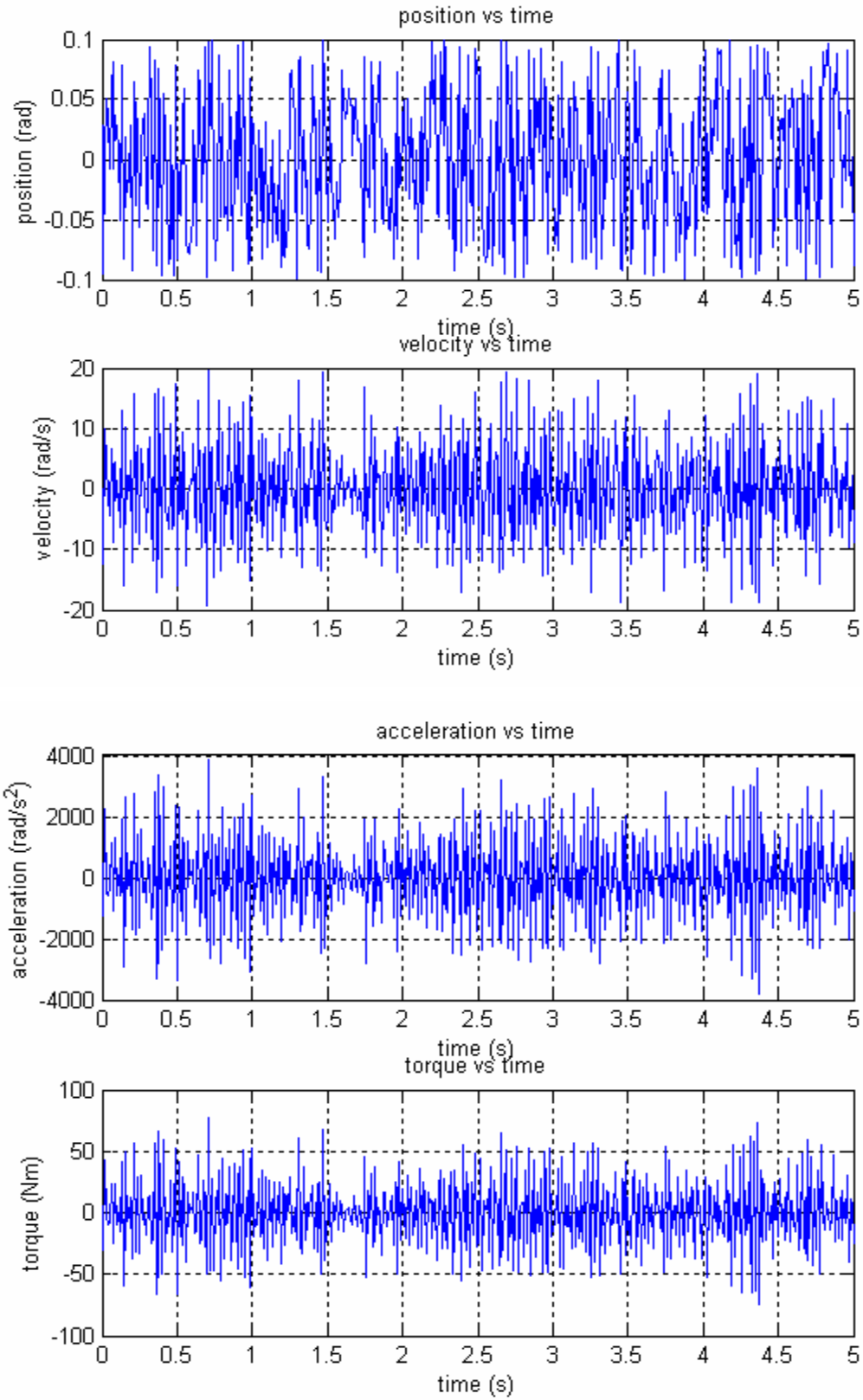


Figure 2.3: Results from simulation of high stiffness case $k = 1000$ Nm/rad.

Case 2: Ankle stiffness ($k=1$)



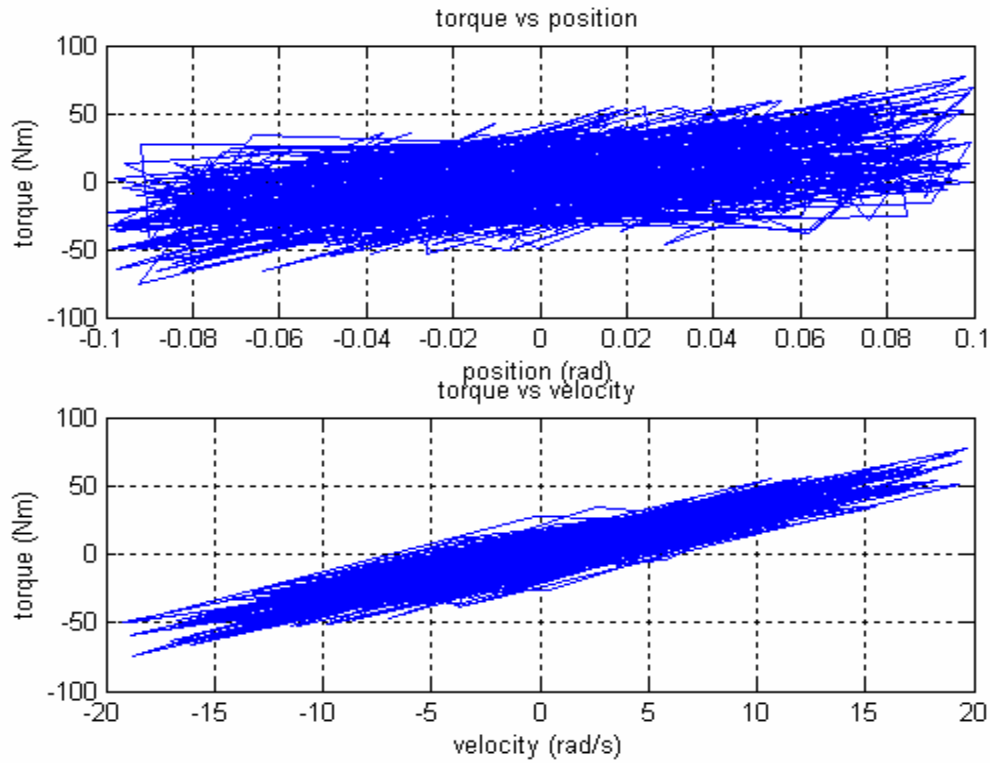
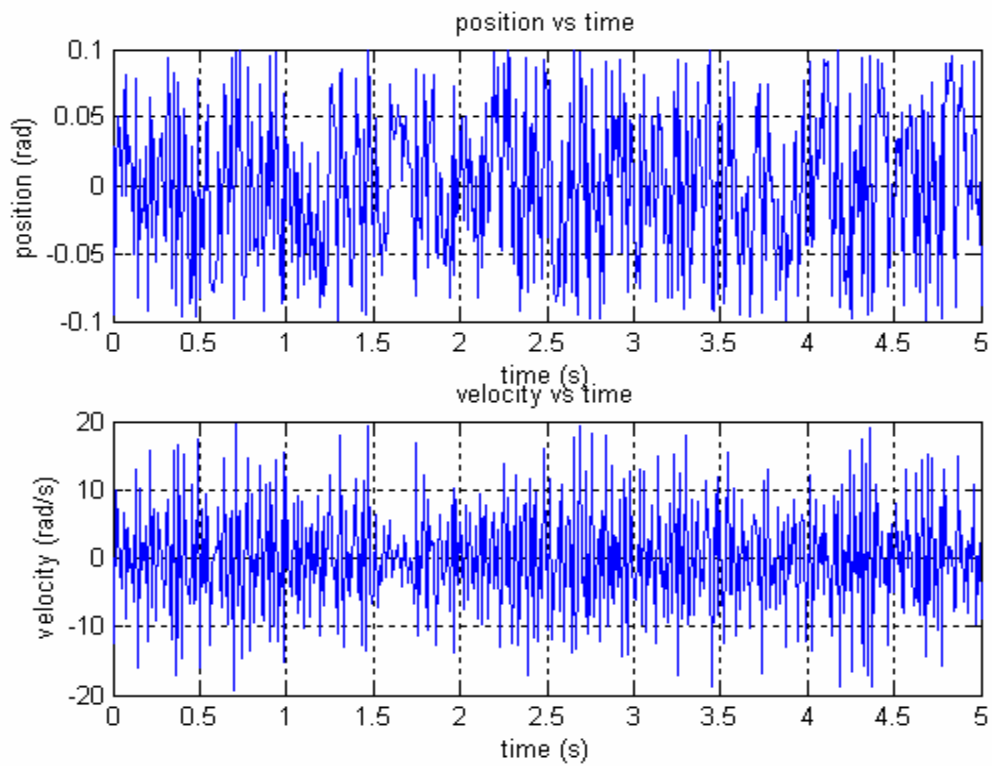


Figure 2.4: Results from simulation of stiffness case $k = 1$ Nm/rad.

Case 3: Ankle with low stiffness ($k=0.01$)



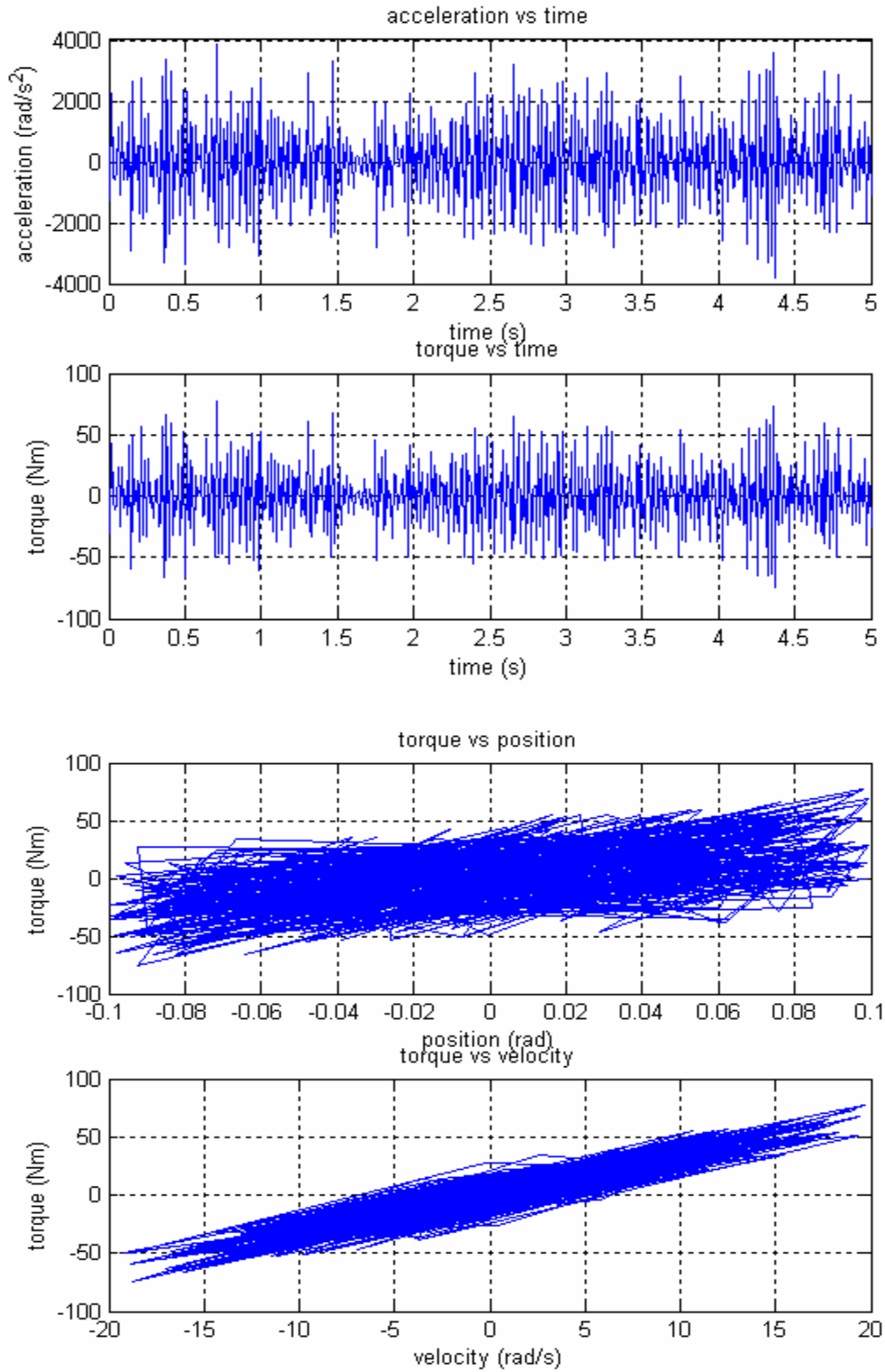
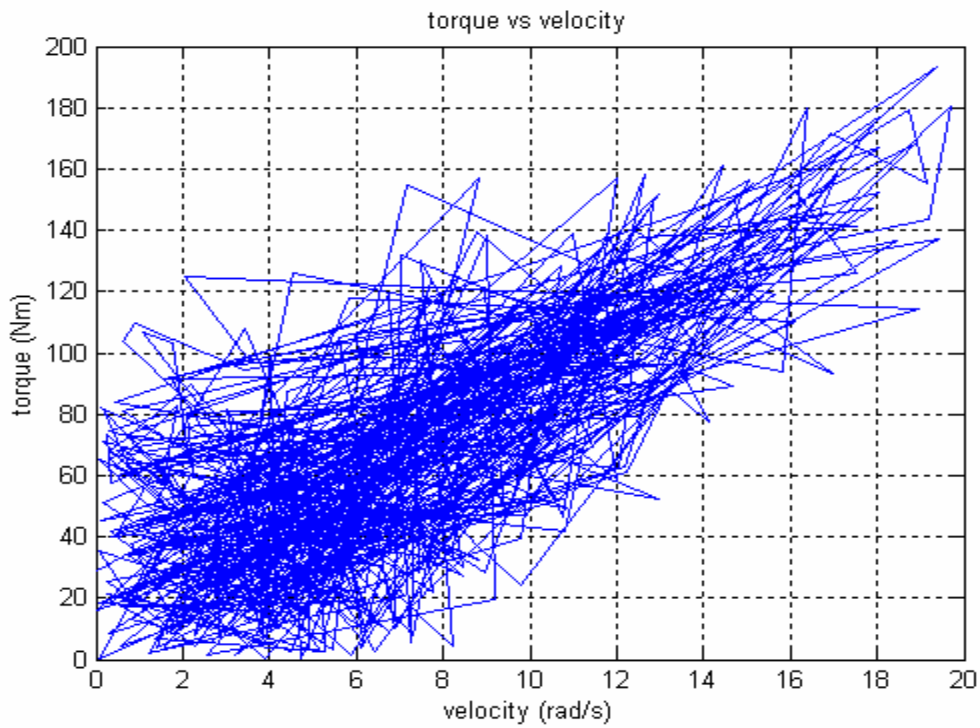


Figure 2.5: Results from simulation of low stiffness case $k = 0.01$ Nm/rad.

Comparison: High stiffness case vs. Low stiffness case

$k = 1000$



$k = 0.01$

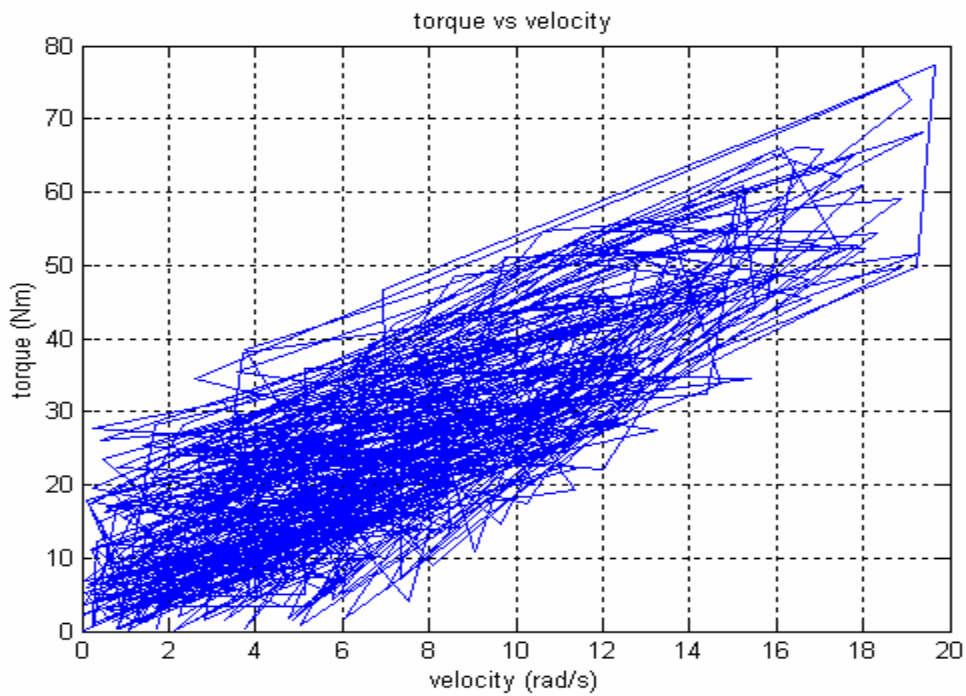


Figure 2.6: Absolute velocity vs. Torque – maximum case and minimum case.

2.3.6 Analysis and Conclusion

The torque velocity limit of the high stiffness case is the maximum case and should be used as the limiting parameters of the actuating system. The maximum velocity reached in the three cases is approximately $v = 20$ rad/s and the maximum torque is approximately $T = 200$ Nm.

The total torque consists of two components: the active torque and involuntary torque due to passive mechanics. Taking the maximum involuntary torque of $T = 200$ Nm with the maximum voluntary contraction to be $T = 150$ Nm, the hydraulic actuator must have a maximum torque of $T_{\max \text{ total}} = 350$ Nm.

Chapter 3

The Design of a Hydraulic Actuating System

Having determined the required performance characteristics of the prospective actuating device, the next step is to employ these criteria in the selection of components and the design of a complete hydraulic actuating system.

3.1 Characteristics of a Hydraulic Actuator

There are certain general characteristics of a hydraulic actuator that make it an ideal motor for this experimental apparatus. In general, the hydraulic actuator has the advantage of a higher torque to inertia ratio resulting in greater accuracy and better frequency response. It has smoother performance at low speeds and is self-cooled, which allows it to operate in stall condition indefinitely without damage. These characteristics meet the needs of this experimental apparatus.

3.2 Hydraulic Actuator System

A hydraulic actuator is an energy-transmitting device that operates on the hydro-mechanical principle. Rotary actuators convert fluid pressure into rotary power, and develop instant torque in either direction. Rotary hydraulic actuators consist of a housing with vanes and a rotating rotor attached to a shaft and inlet and outlet ports for the hydraulic fluid. Differential pressure at the two actuator ports is sensed as a torque across the vanes of a rotary actuator. The amount of output torque developed is determined by the area of the vane, the number of vanes, and the fluid pressure applied. Speed of

rotation is dependent on the flow and pressure capacities of the hydraulic system. Flow to the ports of the actuator is controlled by means of an electrohydraulic servovalve. Flow to and from either port is determined by the spool position which is controlled by the position of the feedback spring. This in turn is determined by the rotation of an electromagnet in a permanent magnetic field. The current in the electromagnet is fed through a servoamplifier unit which operates the system normally in position or velocity feedback modes. A constant pressure variable flow pump mounted in parallel with an accumulator provides flow to the servovalve input port. This is the basic makeup of a hydraulic actuating system.

The design procedure for the hydraulic system is first to select an actuator that is capable of the expected torques, and then from the specifications of the actuator the appropriate servovalve, pump and motor can then be determined.

3.3 Calculations for the Hydraulic Actuating System

The analysis performed in Chapter 2 led to the expected performance requirements of the actuator system. These requirements are listed below.

- Position amplitude: +/- 0.1rad (+/- 6°)
- Maximum velocity: 20 rad/sec
- Maximum acceleration: 4000 rad/sec²
- Maximum torque: 350 Nm (3100 lbf in)
- Required frequency response: 50Hz
- Operating pressure: 20684 Kpa (3000 PSI)

The method to determine the components of the actuator system is to calculate the variables in the hydraulic schematic shown in the figure below. This gives a complete picture of all the variables that interact in this hydraulic system. The hydraulic schematic is shown in Figure 3.0 shown below.

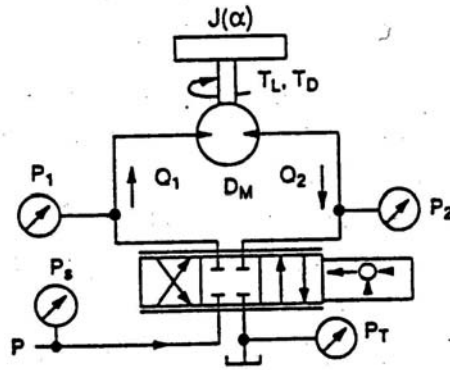


Figure 3.0: Hydraulic schematic of actuator and servovalve.

3.3.1 Calculations for the Actuator

The rotary actuator must overcome the total torque of the hydraulic system. This includes taking into consideration of the inertia of the motor shaft, the damping torque to overcome friction and the total torque required to perturb the ankles as calculated in Chapter 2. The total torque formula is given by Equation 3.0.

$$T = J(\alpha) + T_l + T_d \quad 3.0$$

T = total torque (lbf in)

J = motor shaft inertia (in lbf sec²)

α = angular acceleration (rad/sec²)

T_l = torque required to perturb the ankle-body system (lbf in)

T_d = damping torque to overcome friction (lbf in)

(consider 10% of T_l)

$$T = 0,0062 \text{ lbf} \cdot \text{in} \times 4000 \frac{\text{rad}}{\text{sec}^2} + 3100 \text{ lbf} \cdot \text{in} + 3100 \text{ lbf} \cdot \text{in} \times 10\%$$

$$T \approx 3435 \text{ lbf} \cdot \text{in}$$

Taking the shaft angular velocity of $\alpha = 4000 \text{ rad/s}^2$ and $T_l = 3100 \text{ lbf in}$, the total torque is calculated to be $T = 3435 \text{ lbf in}$. The Textron Micro-Precision hydraulic rotary actuator model 26R2-1V with a motor shaft inertia of $J = 0.0062 \text{ lbf in s}^2$ meets this total torque requirement. The rotary actuator model 26R2-1V develops $T = 3440 \text{ lbf in}$ @ $P = 2000 \text{ PSI}$. The detailed Textron Micro-Precision hydraulic rotary actuator model 26R2-1V specifications are included in the appendix.

3.3.2 Calculations for the Servovalve

To select the servovalve, the following relations are considered. The ideal hydraulic motor provides shaft torque proportional to servovalve differential pressure. The angular speed of the shaft is proportional to servovalve flow [21]. These relations are shown below.

$$P_L = \frac{\pi T_m}{D_m} \quad 3.1$$

$$Q_L = \frac{\omega_m D_m}{2\pi} \quad 3.2$$

T_m = ideal servomotor shaft torque (lbf in)

D_m = servomotor volumetric displacement (in^3/rev)

P_L = load pressure drop (PSI)

ω_m = servomotor shaft speed (rad/s)

Q_L = servovalve load flow rate (in^3/s)

Using Equations 3.1 and 3.2 and taking into account of the total torque, the hydraulic supply pressure, the hydraulic return pressure and the actuator's volumetric displacement, the appropriate servovalve can be determined.

Pressure drops, P_1 and P_2 , are given by Equation 3.3 and 3.4. They are calculated using the total torque found from Equation 3.0, an operational supply pressure of $P = 3000$ PSI and a volumetric displacement $D_m = 1.91$ in³/rad for the above actuator.

$$P_1 = \left(\frac{P_s + P_T}{2} \right) + \left(\frac{\pi T}{D_m} \right) \quad 3.3$$

P_1 = pressure at the port 1 of the servovalve (PSI)

P_s = hydraulic supply pressure (PSI)

P_T = hydraulic return pressure (PSI)

T = total torque (lbf in)

D_m = volumetric displacement of the actuator (in³/rev)

$$P_1 = \frac{3000PSI + 50PSI}{2} + \frac{\pi \times 3435lbf \cdot in}{1.91 \frac{in^3}{rad} \times \frac{2\pi rad}{rev}} = 2424.2PSI$$

$$P_2 = P_s - P_1 + P_T \quad 3.4$$

P_2 = pressure at the port 2 of the servovalve (PSI)

$$P_2 = 3000PSI - 2424.2PSI + 50PSI = 625.8PSI$$

Actual required servovalve flow rate is determined by Equation 3.5 below. Shaft speed is the maximum rotational velocity of 20 rad/s found in Chapter 2 and converted to revolution per minute. Flow is converted into gallons per minute which is standard industry unit for hydraulic systems.

$$Q_L = \frac{N \cdot D_m}{231} \quad 3.5$$

Q_L = servovalve load flow rate (GPM)

N = shaft speed ω_m (RPM)

D_m = volumetric displacement of the actuator (in^3/rad)

$$Q_L = 20 \frac{\text{rad}}{\text{sec}} \times \frac{60 \text{sec}}{\text{min}} \times 1.91 \frac{\text{in}^3}{\text{rad}} \times \frac{1 \text{gal}}{231 \text{in}^3} = 9.9 \text{GPM} \approx 10 \text{GPM}$$

Once the pressure drops and the actual servovalve load flow rate are known, it is possible to determine the size of the servovalve required using Equation 3.6. As standard in the industry, the rated flow of a servovalve is given at $P = 1000$ PSI, the total pressure drop across the valve. The variable restrictions in a servovalve behave like a sharp edged orifice.

$$Q_R = Q_A \sqrt{\frac{500}{P_S - P_1}}$$

Q_R = servovalve's rated flow @ 1000 PSI (GPM)

$$Q_R = 10 \text{GPM} \sqrt{\frac{500 \text{PSI}}{3000 \text{PSI} - 2424.2 \text{PSI}}} = 9.3 \text{GPM} \approx 10 \text{GPM}$$

The appropriate servovalve can now be selected using the calculated rated flow of $Q_R = 10$ GPM. Taking into consideration of the phase lag and the loss of amplitude of the spool position versus the command signal frequency, the Moog high response 2 stage servovalve model 72F599 was selected. Below is a figure of the Moog 72 Series servovalve.



Figure 3.1: Moog 72 Series Servovalve.

A graph of the standard 72 Series performance is illustrated in Figure 3.2 below. The detailed specifications of the Moog 72 Series Servovalve are included in the appendix.

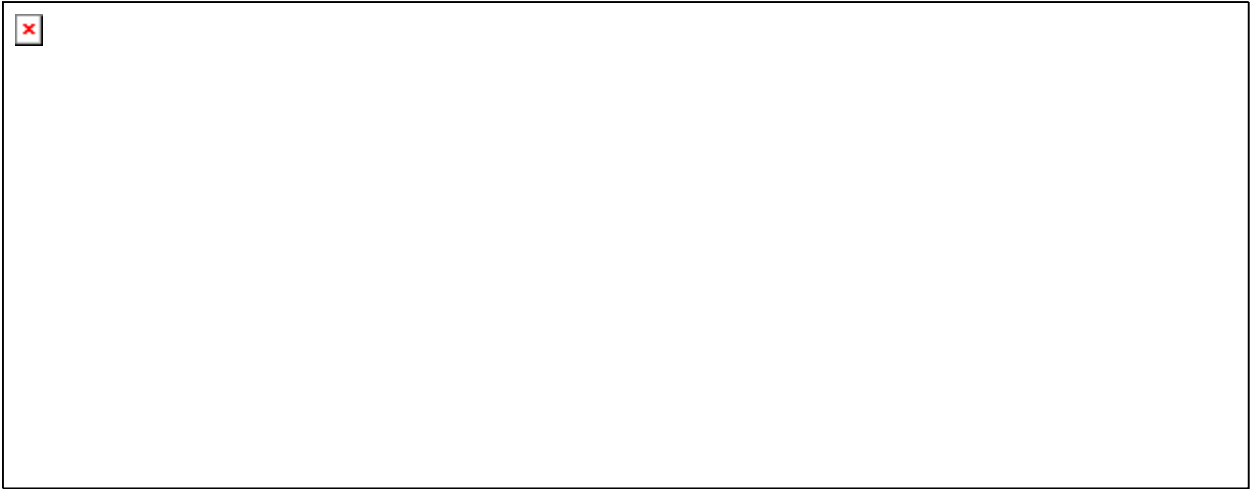


Figure 3.2: Performance graphs of Moog Series 72 Servovalve.

3.4 Conclusion

This chapter covered the selection of the two main components of the hydraulic actuating system: the hydraulic rotary actuator and the servovalve. The actuator selected is the Textron Micro-Precision hydraulic rotary actuator model 26R-2-1V and the servovalve selected is the Moog 72 Series high response servovalve. There will be two sets of these components each used separately to perturb the ankles independently on the apparatus.

Other components of the actuating system are a manifold mounted on each actuator to accept the servovalve, servovalve mating connectors, hydraulic piping and valves for the supply and return of hydraulic fluids.

The selection of the hydraulic pump and motor, which is the other major component of the actuating system, will be covered in Chapter 4.

Chapter 4

Determination of Pump Size

For most Servo-valve Actuator applications the hydraulic pump size is determined by its capability to meet the flow requirements of the maximum system velocity at all times. Due to noise and vibration considerations in the Lyman Duff Building, we want to minimize the pump and motor size yet still meet the performance requirements. This chapter deals with the solution to this optimization problem.

4.1 Discussion of Pump Size and Accumulator

The main determination for the size of a pump supplying hydraulic flow to the servo-valve actuator system is the required velocity of the actuator. The calculations from Chapter 2 revealed that the actuator will reach a maximum velocity of $v = 20$ rad/s. Initially, the specification was for the pump to be able to handle the maximum velocity of $v = 20$ rad/s at all times. But working with the engineer from MCS Servo and Professor Kearney, it was determined that this would be an over design for our application.

The pump and motor for this apparatus will be housed in the basement mechanical room of the Lyman Duff building and piped to the third floor to the REK lab. There are researchers working with microscopes in the floors between. Thus, noise and vibration considerations are important in this design. Our objective is to reduce the pump and motor size as much as possible while still meeting our operational requirements.

The maximum velocity of $v = 20$ rad/s for our system is rarely reached during much of the operation time. As a result, much of the pump's capability is wasted. One way to reduce the size of the pump and motor is to utilize an accumulator. An accumulator is a pressurized vessel that holds hydraulic fluid from the hydraulic supply

on the way to the pump. As the required flow from the actuator goes beyond the capacity of the pump, the accumulator provides extra flow.

4.2 Solution to the Minimization of Pump Size

The solution to this minimization problem is to size the pump for the average velocity of the actuator instead of the maximum velocity. The accumulator will be used to supply the fluid needed to reach the velocities above the average velocity. And it will recharge when the system is operating below the average velocity.

The optimal flow provided by the pump required for the average velocity and the volume of the accumulator must be now determined. The relationship between flow-velocity and volume-position is shown below:

$$\text{Flow (pump)} = \alpha \text{ Velocity} \quad 4.0$$

$$\text{Volume (accumulator)} = \beta \text{ Position} \quad 4.1$$

The velocity of the actuator can be determined by taking the derivative of the position of the actuator.

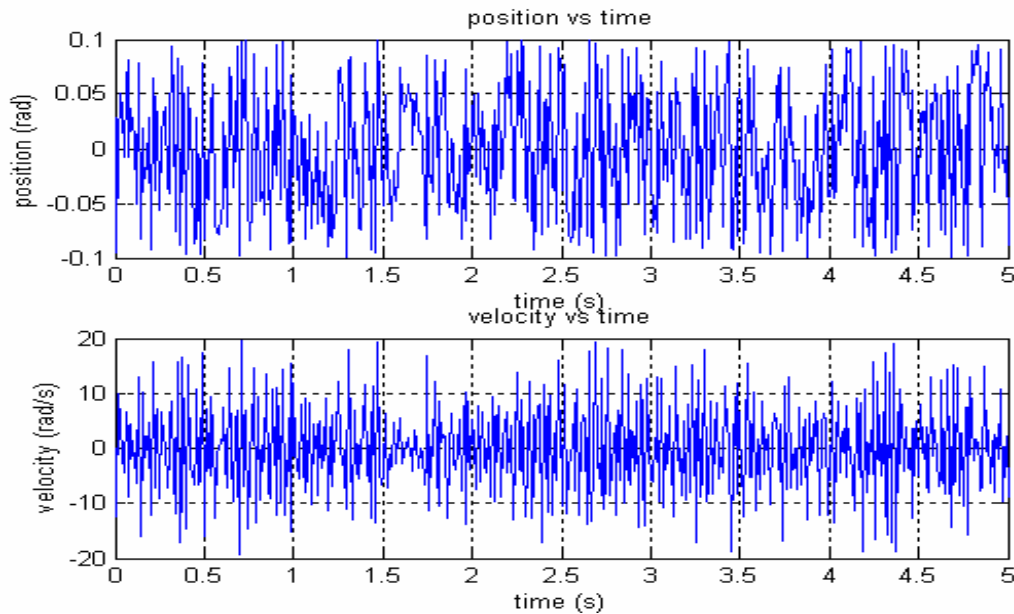


Figure 4.0: Position vs. Time, Velocity vs. Time – Graphs of the actuator.

Above in Figure 4.0 is the position vs. time and velocity vs. time graphs of the actuator.

To determine the average velocity, first take the absolute value of the velocity graph and then find the average velocity over time. The average velocity of the random input was found to be $v = 6.85 \text{ rad/s}$ for our system. To determine the portion of time that the accumulator is being depleted and the portion of time that the accumulator is being charged, the average velocity is subtracted from the absolute value of velocity. In the bottom graph of Figure 4.1, the positive velocities are when the actuator flow is above the capability of the pump and the accumulator is supplying extra flow. The negative velocities are the times when the pump is providing enough flow toward the actuator and is able to charge the accumulator at the same time. The two figures below show the velocity vs. time graphs.

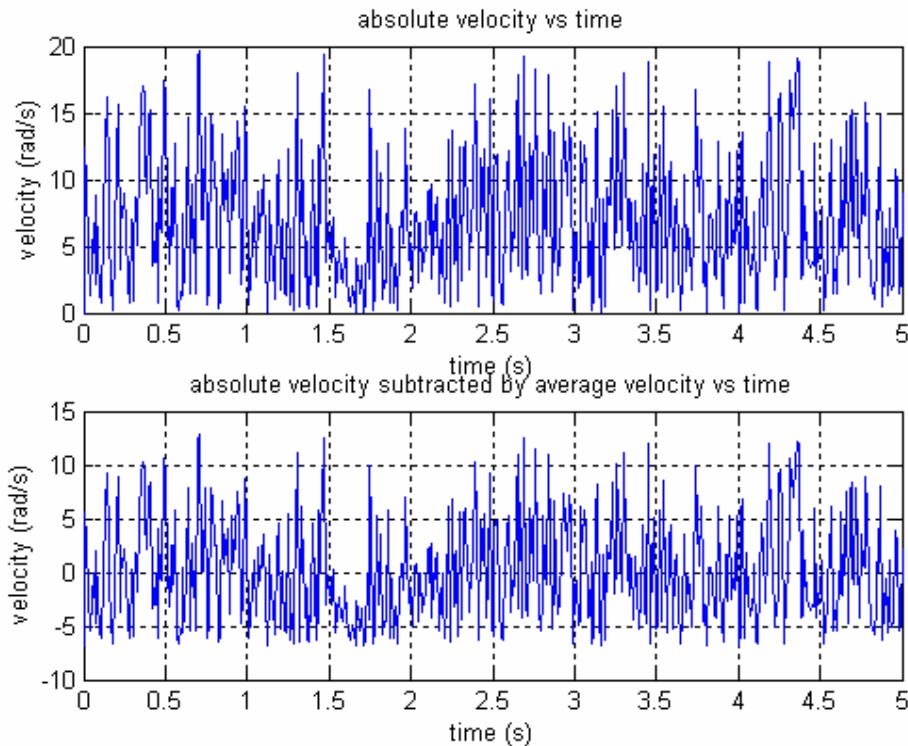


Figure 4.1: Absolute velocity vs. Time and Absolute velocity subtracted by average velocity vs. Time.

The above graphs show the portion of time that the accumulator is being depleted or charged, but does not describe the fluid level or volume of the accumulator. These characteristics can be obtained by integrating the graph of Absolute velocity subtracted by average velocity vs. Time. This graph is essentially the fluid level of the accumulator

through the operation time of the actuator. The accumulator size can be determined by integrating the velocity that is beyond the average velocity, hence the amount of flow above what is provided by the pump. Integration of the velocity function will result in a position function; this position can then be related to the volume of the accumulator as shown in Equation 4.1. Figure 4.2 below shows the Integrated velocity vs. Time graph.

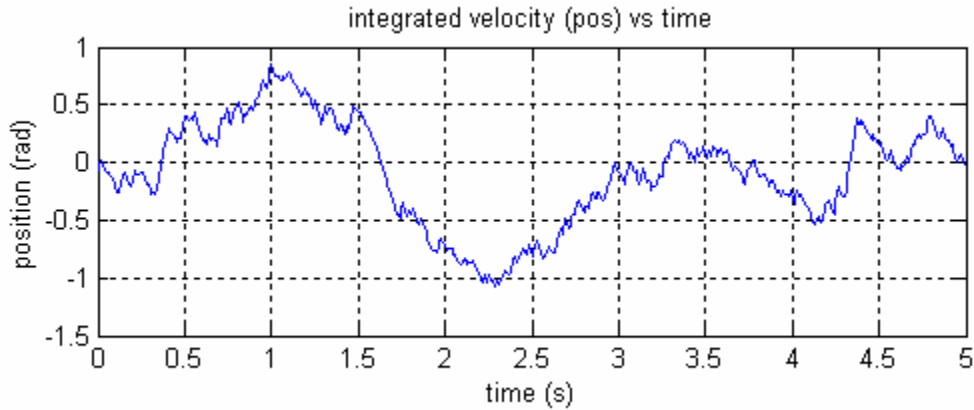


Figure 4.2: Integrated velocity (pos) vs. Time.

4.3 Calculations for the Selection of the Hydraulic Pump

Taking a cautious margin, an average velocity of $v = 10 \text{ rad/s}$ can be used to calculate the flow needed from the pump. The flow that the pump should provide is given by Equation 4.2 below.

$$Q_{\text{pump}} = S \cdot V_d \quad 4.2$$

Q = pump flow (GPM)

S = nominal velocity of the actuator (rad/sec)

V_d = the volumetric displacement (in^3/rad)

$$Q_{\text{pump}} = \frac{10 \text{ rad}}{\text{sec}} \times \frac{60 \text{ sec}}{\text{min}} \times \frac{1,91 \text{ in}^3}{\text{rad}} \times \frac{1 \text{ gal}}{231 \text{ in}^3} = 4.96 \text{ GPM} \approx 5 \text{ GPM}$$

Above is the calculation of the flow needed for the actuator. In addition to the flow required for the actuator the servovalve's internal leakage should also be included. At $P = 3000$ PSI, the internal leakage for the Moog Servovalve model 72F599 is approximately $Q_{Servovalve} = 2.34$ GPM.

$$Q_{Total} = Q_{Pump} + Q_{Servovalve} \quad 4.3$$

$$Q_{Total} = 5GPM + 2.34GPM = 7.34GPM \approx 8GPM \times 2assemblies = 16GPM$$

4.4 Calculations for the Selection of the Electric Motor

The pump requires an electric motor to provide shaft power. The shaft power needed for an operating pressure of $P = 3000$ PSI and a required flow of $Q_{Total} = 16$ GPM is given by the Equation 4.4 below. A safety factor of 85% is included.

$$HP = \frac{Q_{Total} \times P}{1714 \times s.f.} \quad 4.4$$

Q_{Total} = total flow (GPM)

P = operating pressure (PSI)

$s.f.$ = safety factor (%)

$$HP = \frac{16GPM \times 3000PSI}{1714 \times 0,85} = 32,9 \approx 33HP$$

4.5 Conclusion

The above calculations for the pump and electric motor led to the selection of a 21GPM Rexroth pump adjusted at 3000 PSI and a 40 HP electric motor running at 1800 RPM. This is a significant reduction of pump and motor size from the original calculations and a cost savings of \$2600.00. This will be the hydraulic power supply for

the apparatus. The calculations above were completed with the help of Benoit Fortin, engineer from MCS Servo.

Chapter 5

The Design of Auxiliary Components

This Chapter discusses the selection and design of the various auxiliary components of the apparatus. Some components were selected from available products others were custom designed.

5.1 List of Components

The auxiliary components described in this chapter are:

1. Torque transducer
2. Potentiometer
3. Mechanical and electrical stops
4. Bearings
5. Foot pedals
6. Couplings between components

The mechanical drawings of these components are given in the appendix.

5.2 Torque Transducers

The torque transducer selected for this apparatus is the Lebow Products Flanged Reaction Torque Sensor, Model 2110-5K from Intertechnology Inc. of Montreal. This reaction torque transducer is made for mounting directly to drive shafts of test

applications, which is the method that we will mount this torque transducer. The torque transducer is connected on one side to the bracket mounted to the foot. The other side of the torque transducer is connected to the drive shaft of the hydraulic actuator. The torque transducer will measure the ankle joint torque. The Lebow Torque Transducer model 2110-5K has a rated capacity of $T = 565 \text{ Nm}$ (5000 lb.in.) which allows it to withstand the maximum combined torque due to voluntary contraction and passive mechanics. The maximum combined torque calculated in Chapter 2 was $T_{Total} = 350 \text{ Nm}$. Some other characteristics of the torque sensor is a high torsional stiffness of 103941 Nm/rad, a high resistance to bending moments, minimal friction error, and low-end force sensitivity due to the absence of moving parts. The torque transducer is shown below in Figure 5.0 and the detailed specifications can be found in the Appendix.



Figure 5.0: Lebow Torque Transducer 2110-5K.

5.3 Potentiometer

The position feed back of this apparatus is provided by a rotary potentiometer. The selected potentiometer is from Maurey Instrumentation Corporation model 112-P19 1 watt solid molded element conductive plastic potentiometer. The potentiometer operates with a variable resistance conductive plastic strip around the axis; as the potentiometer rotates the resistance changes. This provides a position feed back for the control system. The potentiometer specifications are provided in Appendix.



Figure 5.1: Maurey Instrumentation model 112-P19 potentiometer.

5.4 Mechanical and Electrical Stops

The position of the rotary actuator is controlled by the input displacement signals of the control software. This type of position control may be adequate for most applications, but due to the fact that this machine will be used to conduct experiments on humans there must be multiple safety backups. On this apparatus there is a mechanical stop and an electrical stop to limit shaft rotation within the free range of motion of the ankle as a measure of safety.

The mechanical stop consists of a cam shaped disk that also acts as a coupling between the motor and torque transducer. The disk rotation is limited by two steel arches that are mounted parallel to the disk and on either side of the cam head. The arches are sandwiched between two circular fixed flanges. The angular location of the arches on the flanges can be varied in increments by virtue of boltholes on the flanges covering a rotation of 180°. This type of mechanical stop has been utilized successfully on other similar hydraulic actuating systems in the lab.

The design of the mechanical stop frame includes a shelf for supporting the standing platform and a protrusion for mounting to the base plate. The protrusion mounting design allows for the disassembly of the stop mechanism from above, without the need to access the bottom of the base plate. The frames are made from steel while the cam is made from aluminum to reduce the mass and decrease the rotational inertia of the drive shaft. The mechanical stop is shown below in Figure 5.2.

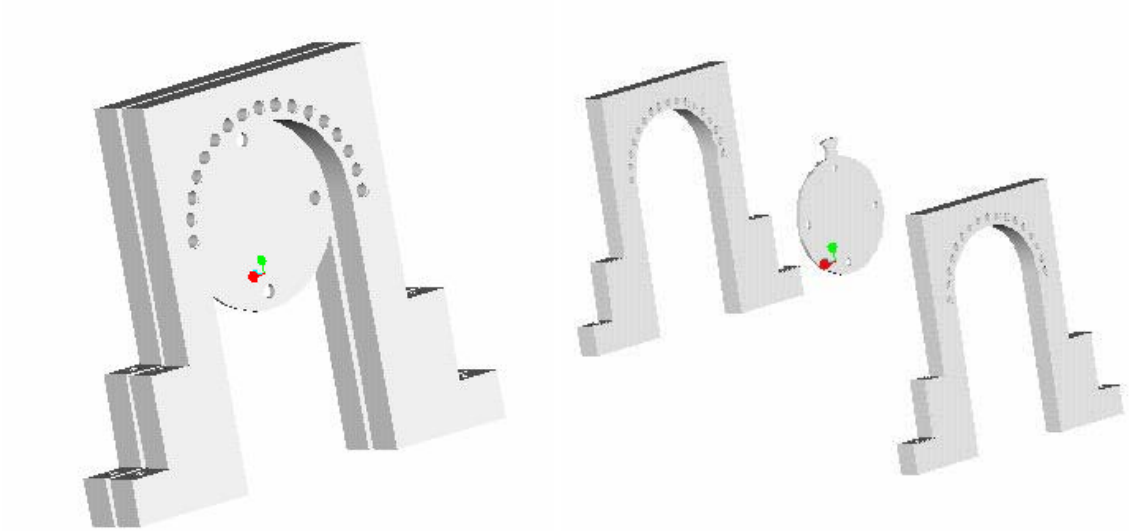


Figure 5.2: Isometric and exploded views of the mechanical stop assembly.

The electric stop consists of a linear sensor mounted on the connecting box between the rotary actuator, the servovalve and the hydraulic supply pipes. A cam is connected to the drive shaft of the actuator following its movement. The length of the arc of the groove on the cam is the range of rotation to be limited. The cam is actually constructed of two plates with each plate containing one side of the cam. This construction allows the adjustment of the range of motion by rotating the plate thereby changing the arc length of the groove. The linear sensor follows the cam and activates the electric stop once the cam moves out of the groove. The electrical stop shuts off the hydraulic supply stopping any further change in position.

A third safety stop is a handheld stop button for the person being experimented on. The button stop is connected to the switch valve of the hydraulic supply pipe coming out of the accumulator. A press of the stop button switches the valve and reroutes the hydraulic supply away from the actuator and to the return pipe. The effect is an immediate shutoff of the hydraulic actuator. This can be used at anytime during the operation of the apparatus if the person senses any danger or discomfort. This is only a rerouting of the hydraulic supply; the pump meanwhile remains in operation. These three safety stops are part of an overall safety design to ensure safe operation of the apparatus.

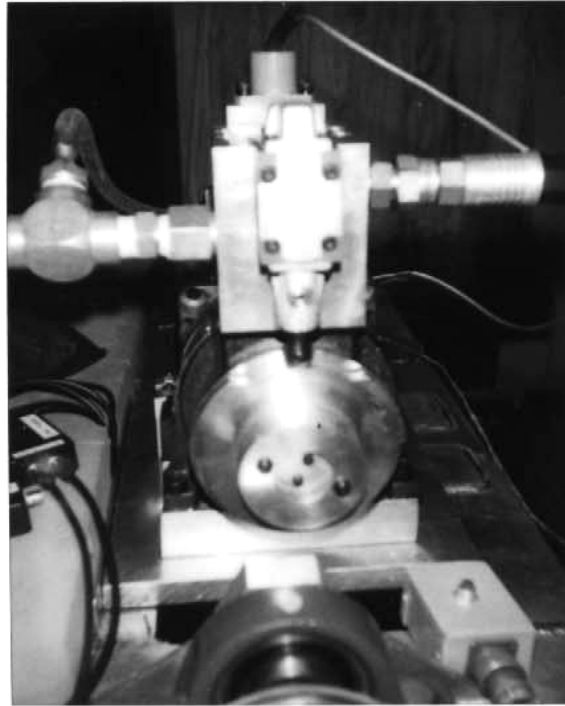


Figure 5.3: Picture of the linear sensor, cam and stop button.

5.5 Bearings

The bearings are mounted on either side of the foot mount bracket to facilitate the rotation of the shaft. The bearings will not be subjected to significant axial or radial stress; their main function is to prevent the lateral vibration of the shaft. Thus it was not necessary to obtain special bearings made to accommodate radial and axial stresses. The type of bearing that was chosen are deep groove ball bearings purchased from General Bearings in Montreal. The bearings are SKF model 6010-2RS1 with inside diameter $D_i = 50$ mm and width $W = 15$ mm.

5.6 Foot Pedal and Bracket

The foot pedal bracket is constructed from three rectangular plates forming a U-channel. The two vertical side plates are connected to the shafts passing through the

bearings and connected to the rotary actuator. The central plate has two slots for the bolts for mounting the foot pedal or moulded foot boot. There are two types of foot mount for this experimental apparatus. The first is a flat aluminum plate on which the person being tested on will simply place their foot. The second is a fiberglass boot custom made for each person. A fiberglass cast is made of the foot to ensure proper and exact fitting. Metal stems are attached to the fiberglass boot at the ankle joint and mounted on the bracket. This foot bracket is designed to be able to accommodate the same fiberglass boot as the other experimental apparatus currently in the REK Lab. The entire assembly is constructed of aluminum material in order to reduce the mass and minimize rotational inertia. The foot bracket with the flat aluminum pedal is shown below in Figure 5.4.

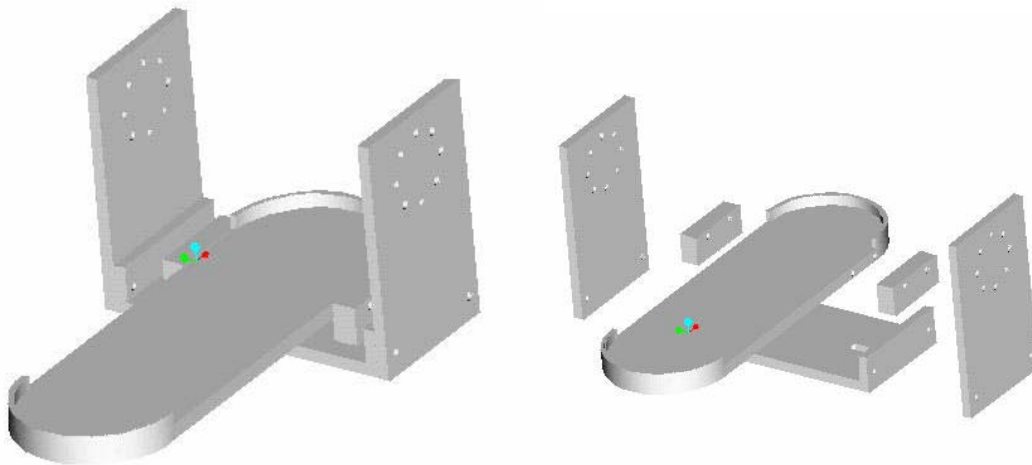


Figure 5.4: Isometric and exploded view of the foot bracket and pedal.

5.7 Couplings

Two couplings were custom designed for this apparatus. One coupling is connects the actuator shaft to one face of the mechanical stop rotor. The second coupling connects the torque sensor to the foot bracket.

The coupling between the torque transducer and the foot bracket consists of a two-section shaft. The larger diameter section is attached to the transducer using 4 M8 × 30 bolts, and the small diameter section is passed through the bearing and attaches to the foot pedal using 8 M4 × 15 screws. The coupling is shown in Figure 5.5.

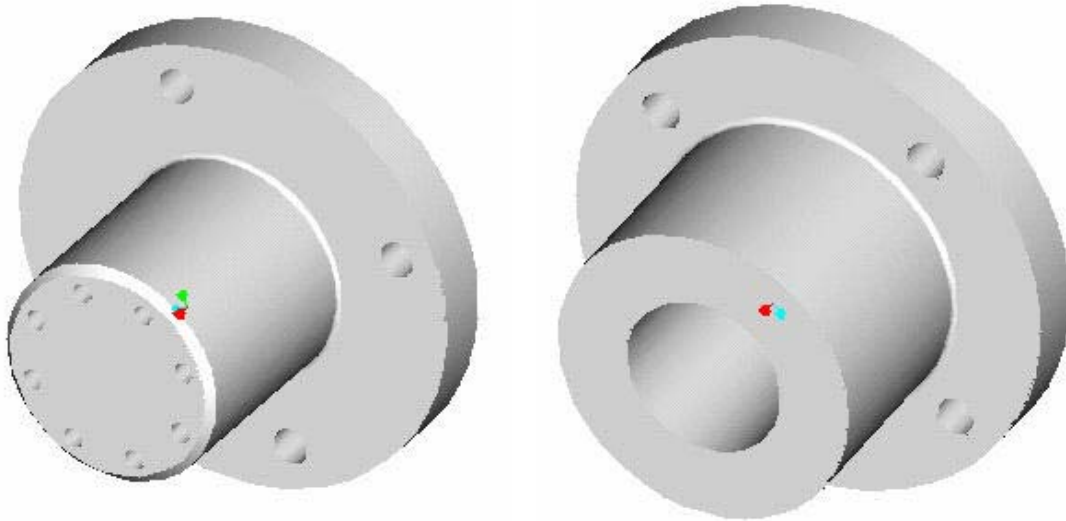


Figure 5.5: Torque sensor coupling.

Figure 5.6: Actuator coupling.

The coupling between the actuator is also a two-section shaft. The larger diameter section is attached to the mechanical stop rotor and using 4 M8 × 30 bolts. The smaller diameter section is attached to the spline shaft type T26. Both couplings are made using aluminum to reduce rotational inertial of the drive shaft. The coupling is shown in Figure 5.6.

Chapter 6

The Design of the Apparatus Structure

This chapter deals with the overall design of the apparatus, including the different elements of the apparatus, the support frames, the subassemblies and the final assembly.

6.1 The Overall Design

The objective of the design is to design an apparatus for the measurement of the dynamic ankle joint stiffness of humans in upright stance. The frame and supporting components must house the actuating system, the torque sensor and the potentiometer in the manner that will satisfy this goal.

The design philosophy for this apparatus is a modular design approach. The different components and subassemblies are mounted on a base. The subassemblies can be removed or repositioned as needed without affecting the other parts of the machine. Platforms and safety handlebars must also be incorporated in the design for human testing. This chapter will detail the designs of the following elements:

1. Support flanges
2. Base
3. Subassembly with actuator, torque sensor and foot bracket
4. Whole assembly with foot platform and handrail

6.2 Support Flanges

The flanges support the drive shaft and the weight of the torque sensor, foot bracket and the weight of the person being tested. The flanges house the bearings, which facilitate the rotation of the shaft coupling and minimize vibration. The support flanges are made with steel and is shown in Figure 6.0.

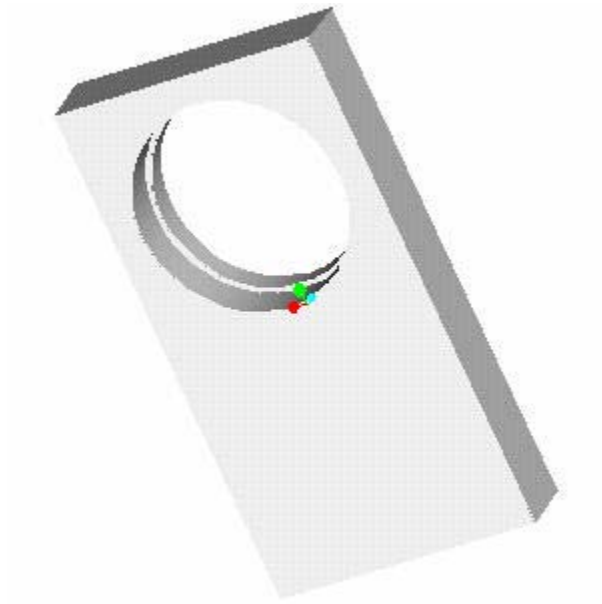


Figure 6.0: Isometric view of support flange.

6.3 Base

The base component is the foundation of this apparatus. This part will support the subassemblies of the actuator system, and the hand railings. The base will be constructed of standard tubular 3 × 4 inch steel beams that will be cut to customized lengths and welded together. The base is shown in the Figure 6.1 below.

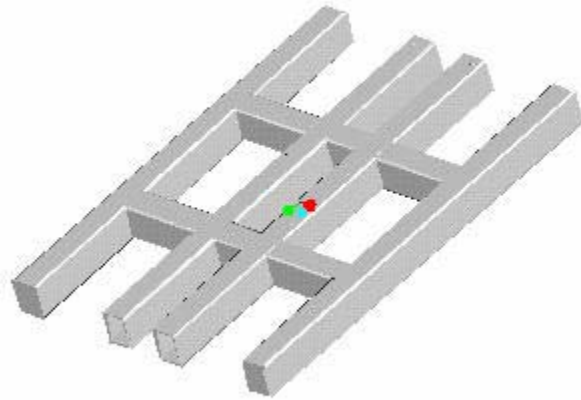


Figure 6.1: Isometric view of base component.

6.4 Subassembly with Actuator, Torque sensor and Foot bracket

The subassembly with actuator, torque sensor and foot bracket is a major module of the apparatus. It contains all the important components including the potentiometer, the torque sensor, the foot bracket, the mechanical stop and the actuator assembly. This modular design allows the removal of the entire subassembly for repair or upgrade. Another function of this modular design is the ability to adjust the spacing between the two feet to accommodate the different dimensions of the people being tested. There are four slots machined on either side of one base plate to accommodate four bolts attached to the base. This design allows the entire assembly to be shifted along these slots. The spacing between the two feet can be adjusted from a range of 10 inches to 16 inches measured from mid-foot to mid-foot. There are two similar subassemblies for machine, one has a base plate with the four slots and the other has just four holes for permanent mounting to the base. The base plates are constructed from aluminum to reduce weight and prevent rusting. The subassembly is shown below in Figure 6.2.

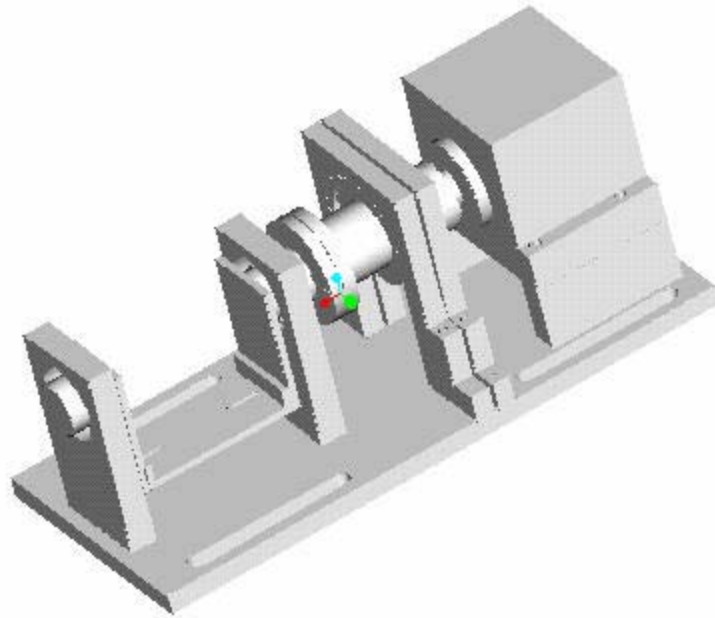


Figure 6.2: Isometric view of subassembly.

6.5 Whole Assembly with Foot Platform and Handrail

The final assembly is essentially a flat platform with two holes housing the two foot pedals. The person being tested will be standing on the foot pedals. The platform around the foot pedal is used for stepping onto or off the pedals. The platform is bolted on to the subassembly structure and it will shift together with the base platform. A railing mounted to the base supports the other side of the platform.

There will be a protective shield around the hole that will follow the path of the foot pedal that will block the space between the pedal and the platform. This is a protective measure to make sure that toes are not crushed between the pedal and platform. The handrail is another safety device for balance support while stepping onto and off the foot pedals and for support during the operation of the apparatus.

Due to the fact that the axis of rotation of the ankle is above the flat of the foot, some components of this apparatus protrude above the foot platform. This could be a

dangerous hazard if the person being tested falls onto these components. A protective cover will be mounted on the foot platform to cover these components as a safety measure.

Vibration absorbing mounts will be set along the bottom of the base to absorb the mechanical vibrations and establish a stable operating environment.

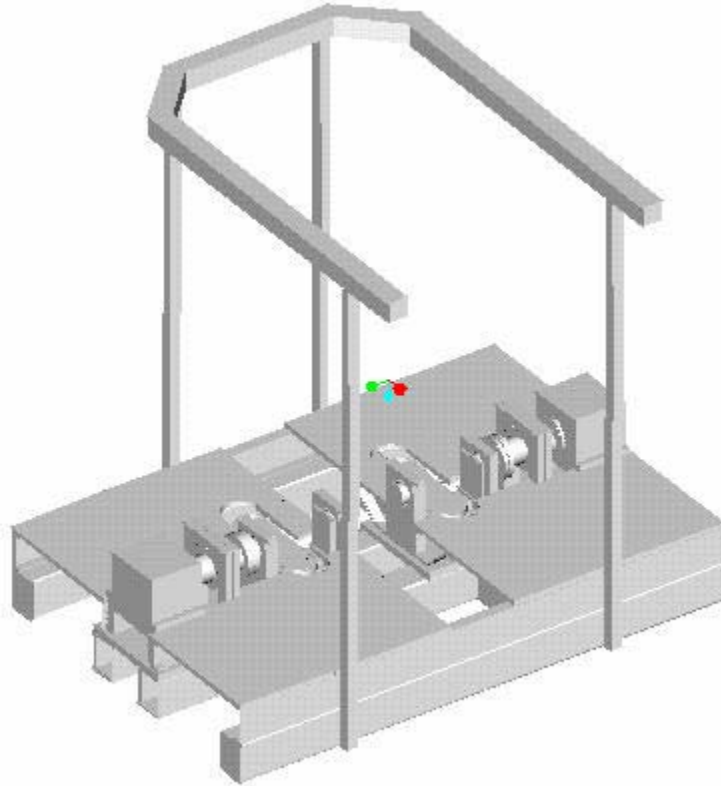


Figure 6.3: Isometric view of final assembly.

The assembly drawings of the apparatus and its parts will be included in Appendix.

References

1. Inman, V.T., *The Joints of the Ankle*. 1976, Baltimore: Williams and Wilkins.
2. Bottlang, M., J.L. Marsh and T.D. Brown, *Articulated External Ankle Fixation: Optimal Axis Alignment to Minimize Motion Resistance*, Proceedings of the North American Congress on Biomechanics, Waterloo, Ontario, 1998. August.
3. Nasher, L.M., et al., *Organization of postural controls: An analysis of sensory and mechanical constraints*. Progress in Brain Research, 1989. **80**: p.411-418.
4. Nasher, L.M. and G. McCollum, *The organization of human postural movements: A formal basis and experimental synthesis*. Behavioural Brain Sciences, 1985. **8**(135-172).
5. Kearney, R.E., *System identification of the functional modulation of intrinsic and reflex stiffness*. Research Module 5.9, 1999.
6. Fitzpatrick, R.C., et al., *Postural proprioceptive reflexes in standing human subjects: bandwidth of response and transmission characteristics*. Journal of Physiology, 1992. **458**: p.69-83.
7. Fitzpatrick, R.C., J.L. Taylor, and D.I. McCloskey, *Ankle stiffness of Standing humans in response to imperceptible perturbation: reflex and task-dependent components*. Journal of Physiology, 1992. **454**: p.533-47.
8. Fitzpatrick, R., D. Burke, and S.C. Gandevia, *Task-dependent reflex responses and movement illusions evoked by galvanic vestibular stimulation in standing humans*. Journal of Physiology, 1994. **478**(Pt2): p.363-72.
9. Young, R.R., *Spasticity: a review*. [Review]. Neurology, 1994. **44**(11 Suppl 9): p.S12-20.
10. Surial, A.L., *Design of a compact clinical device to measure dynamic ankle mechanics*. McGill University, 1988.
11. Hoffer J.A. and S. Andreassen, *Regulation of soleus muscle stiffness in premammillary cats: intrinsic and reflex components*. J. Neurophysiol., 1981. **45**: p.267-285.
12. Nichols, T. and J. Houk, *Improvement in linearity and regulation of stiffness that results from actions of stretch reflex*. Journal of Neurophysiology. 1976. **29**: p.119-142.

13. Carter, R.R., P.E. Crago and M.W. Keith, *Stiffness regulation by relex action in the normal human hand*. Journal of Neurophysiology, 1990. **64**: p.105-118.
14. Crago, P.E., J.C. Houk, and Z. Hasan, *Regulatory actions of human stretch reflex*. Journal of Neurophysiology, 1976. **39**(5): p.925-35.
15. Feldman, A.G., *Functional tuning of nervous system with control of movement or maintenance of a steady posture*. II. Controllable parameters of a muscle. Biophysics, 1966.**11**: p.567-578.
16. Feldman, A.G., *Change in length of the muscle as a consequence of a shift in the equilibrium in the muscle-load system*. Biophysics, 1974. **19**: p.544-548.
17. Hogan, N., *An organizing principle for a class of voluntary movements*. Journal of Neuroscience, 1984. **4**: p.2745.
18. Hunter, I.W. and R.E. Kearney, *Dynamics of human ankle stiffness: variation with mean ankle torque*. Journal of Biomechanics, 1982. **15**: p.747-752.
19. Agarwal, G.C. and G.L. Gottlieb, *Oscillation of the human ankle joint in response to applied sinusoidal torque on the foot*. Journal of Physiology, 1977. **268**: p.151-176.
20. Gottlieb GL, G.C. Agarwal, R.D. Penn: *Sinusoidal oscillation of the ankle as a means of evaluating the spastic patient*. J Neurol Neurosurg Psychiatry 41:32-39, 1978
21. Clark, D.C., *Selection and performance criteria for electrohydraulic servodrives*. Moog Inc., East Aurora, New York.

Appendix

Appendix contains detailed specifications of the following components:

1. Potentiometer
2. Torque Transducer
3. Servovalve
4. Hydraulic Actuator
5. CAD Assembly Drawings of the Apparatus

